



# Overview of Hierarchical Models for Hyperspectral Image Classification

Yuliya Tarabalka

## ► To cite this version:

Yuliya Tarabalka. Overview of Hierarchical Models for Hyperspectral Image Classification. UkrO-BRAZ - Signal/Image Processing and Pattern Recognition Conference, Oct 2012, Kyiv, Ukraine. pp.1-4. hal-00752928

**HAL Id: hal-00752928**

**<https://hal.inria.fr/hal-00752928>**

Submitted on 16 Nov 2012

**HAL** is a multi-disciplinary open access archive for the deposit and dissemination of scientific research documents, whether they are published or not. The documents may come from teaching and research institutions in France or abroad, or from public or private research centers.

L'archive ouverte pluridisciplinaire **HAL**, est destinée au dépôt et à la diffusion de documents scientifiques de niveau recherche, publiés ou non, émanant des établissements d'enseignement et de recherche français ou étrangers, des laboratoires publics ou privés.

# Overview of Hierarchical Models for Hyperspectral Image Classification

Yuliya Tarabalka

INRIA, AYIN team  
06902 Sophia Antipolis, France  
yuliya.tarabalka@inria.fr

## Abstract

Hyperspectral imaging enables accurate classification, but also presents challenges of high-dimensional data analysis. While pixelwise classification methods classify each pixel independently, recent studies have shown the advantage of considering the correlations between spatially adjacent pixels for accurate image analysis. This paper provides an overview of the available hierarchical models for spectral-spatial classification of hyperspectral images. The two most recent models are experimentally compared on a 102-band ROSIS image of the Center of Pavia, Italy. The experimental results demonstrate that classification methods using hierarchical models are attractive for remote sensing image analysis.

## 1. Introduction

Classification of remote sensing images is an important and challenging task in many application domains, such as precision agriculture, mineralogy, and monitoring and management of environment. The objective of the *image classification* system is to categorize each pixel or each object in the image into one of the information classes that characterize the analyzed scene. The advent of hyperspectral imagery has opened new possibilities in image analysis and classification. *Hyperspectral imaging* sensors measure the energy of the received light in tens or hundreds of narrow spectral channels in each spatial position [1]. Consequently, it becomes possible to identify physical materials and objects within the image scene with higher accuracies when compared to panchromatic or multispectral images. However, when classifying hyperspectral images, two principal challenges must be addressed: 1) data processing in a high-dimensional spectral space; 2) extraction and analysis of spatial information.

A wide range of *pixelwise* classification methods have been proposed, which assign to each pixel a class based on its spectrum. One of the most accurate and frequently used techniques is a kernel-based Support Vector Machines (SVM) classifier, which has good generalization ability and performs well on a high-dimensional data, when a limited number of samples is available [2].

Recent works have shown the advantage of includ-

ing information about spatial dependencies for accurate classification, i. e. performing *spectral-spatial* classification [3, 4]. One of the approaches of spectral-spatial classification consists in including the information from the closest neighborhood for classifying each pixel, using for instance morphological operators [5] or Markov random fields [6]. Even though classification accuracies were improved when compared to pixelwise classification, the use of these methods raises the problem of neighborhoods' scale selection.

Another group of spectral-spatial classification techniques applies segmentation for defining spatial dependencies in the image [4]. Segmentation partitions an image into homogeneous regions with respect to some homogeneity criterion. The challenge consists in selecting an appropriate measure of region homogeneity. This paper gives an overview of hierarchical segmentation models developed for spectral-spatial classification of hyperspectral images. An hierarchical optimization method starts with initial image partitioning or considers each pixel as one region, and iteratively merges the most similar adjacent regions [7]. A measure of region similarity and a convergence criterion must be defined. The paper reviews the selection of these criteria in the available hierarchical models, and explains how spatial dependencies are exploited for accurate classification.

The paper is organized as follows. In the next section, an overview of hierarchical models for hyperspectral image classification is given. The two most recent models are experimentally compared in Section 3. Finally, conclusion is drawn in Section 4.

## 2. Hierarchical models for hyperspectral image classification

### 2.1. Multilevel context-based model

Bruzzone and Carlin [3] were the pioneers in exploiting hierarchical analysis for context-based classification of high-resolution remote sensing images. In order to mitigate the dependence of segmentation performance on the convergence criteria, they proposed to use a set of partitions, or levels, obtained by hierarchical region growing. For each given pixel  $\mathbf{x}$  and at each level  $l$ , a region

to which this pixel belongs defines the spatial context of this pixel.

The multiresolution segmentation algorithm starts from the pixel level, where each pixel represents a region. At each iteration, regions are merged into bigger ones. The aim is to minimize the homogeneity predicate when two regions are merged. This predicate is defined as a cost criterion for the fusion of two regions, and it takes into account spectral and shape (compactness and smoothness) constraints. If the smallest growth of the merging cost exceeds a threshold defined by the user, the region merging process at the considered level  $l$  converges. The number of levels must be chosen by the user, and it mainly depends on: 1) geometrical resolution of the image and 2) size of the objects present in the scene.

Once multilevel segmentation is performed, context-based features are computed for each pixel (mean, standard deviation, area, shape factor at each segmentation level) and are stacked into one vector. SVM classification using these feature vectors is further performed.

Good classification performances on panchromatic remote sensing images were reported. Huang and Zhang recently applied a similar approach for classification of hyperspectral data, by using the spectral cost criterion as a homogeneity predicate [8]. Because the dimensionality of the resulting feature vector is significant, the multilevel hierarchical model is computationally and space expensive.

## 2.2. SVM classification of segmentation regions

Linden et al. [9] applied SVM for classification of every region in a hyperspectral image. First, *eCognition* region growing segmentation is performed [10]. It starts with individual pixels as the initial regions, and at each iteration it randomly distributes subsequent merges as far as possible from each other over the whole image. The dissimilarity criterion between regions is computed as a linear combination of radiometric heterogeneity, computed as the mean of the variance in each spectral channel, and form heterogeneity, computed as the ratio between the actual edge length of a segment and the edge length of a square with the same number of pixels as the segment. The user must select relevant segmentation level(s).

Then, a vector mean for every region is computed, such that the value in each band represents the average spectral information of the pixels in the considered region in the respective band. Afterwards, the regions are classified by an SVM classifier. The obtained experimental results were generally not an improvement over those obtained by pixelwise classification. The possible reason may lie in the fact that a vector mean is a poor representative feature for image regions.

Tarabalka et al. [11] proposed a *majority vote* approach to overcome this drawback. In their method, first

Hierarchical Segmentation (HSeg) is performed. It iteratively merges the closest adjacent regions according to the Spectral Angle Mapper (SAM) criterion, and includes a possibility of merging non-adjacent regions by spectral clustering. An appropriate level of segmentation detail can be chosen interactively with the software HSEGVIEWER. Then, SVM pixelwise classification of the image is performed. Finally, for every region in the segmentation map, all the pixels are assigned to the most frequent class within this region. The described technique yielded a significant improvement of classification accuracies when compared to methods using local spatial neighborhoods. However, in [11] a method for the automated selection of relevant hierarchical level(s) was not proposed.

## 2.3. Marker-based hierarchical segmentation

In [4], Tarabalka et al. proposed a marker-based method for the automated selection of a single hierarchical segmentation level. A marker is defined as a set of image pixels associated with one object. The marker-controlled segmentation approach determines a marker for each object and then segments an image in such a way that each region in a segmentation map contains one marker. The authors proposed to use probabilistic classification results for selecting the most reliably classified pixels as markers of spatial regions.

First, probabilistic SVM classification of a hyperspectral image is performed. This step results in a classification map, where each pixel has a class label, and a probability map, where each pixel contains a probability estimate to belong to the assigned class. A connected components labeling is further applied on the classification map. Each connected component is analyzed as follows:

- If a region is large (number of pixels in the region  $> M$ ), its marker is defined as the  $P\%$  of pixels within this region with the highest probability estimates.
- If a region is small, its potential marker is formed by the pixels with probability estimates higher than the defined threshold  $S$ .

The main idea behind the Marker-based HSeg (M-HSeg) method consists in assigning a marker label for each region containing marker pixels, and iteratively merging regions with an additional condition: two regions with different marker labels can not be merged together. The SAM or other dissimilarity criterion can be used for region growing. The iterative process stops when a number of regions is equal to the number of markers, and hence no more merging is possible. Finally, the class of each marker is assigned to all pixels in the region containing this marker. The drawback of the marker-based hierarchical model is that the final classification result strongly depends on the performances of the marker selection procedure.

## 2.4. Hierarchical segmentation with integrated classification

For mitigating the drawback mentioned in the previous subsection, Tarabalka and Tilton [12] proposed a Hierarchical Segmentation with integrated Classification (HSegClas) model for hyperspectral imagery. The method proceeds as follows:

First, SVM pixelwise classification is performed, resulting in a classification map and  $K$  class probabilities for each pixel for a  $K$ -class problem. At the next step, hierarchical segmentation with integrated classification is performed using the following procedure:

1) Assign a new region label for each pixel. Each new region  $R_i$  gets a preliminary class label  $L(R_i)$  and a  $K$ -dimensional vector of class probabilities  $\{P_k(R_i) = P(L(R_i) = k|R_i), k = 1, \dots, K\}$ .

2) Calculate the dissimilarity criterion  $DC(R_i, R_j)$  between all pairs of spatially adjacent regions  $\{R_i, R_j\}$  as a function of statistical, classification and geometrical features:

- First, the spectral dissimilarity  $DC_{spec}(R_i, R_j)$  between two regions is estimated by computing SAM between the region mean vectors  $\mathbf{u}_i = (u_{i1}, \dots, u_{iB})^T$  and  $\mathbf{u}_j = (u_{j1}, \dots, u_{jB})^T$ :

$$DC_{spec}(R_i, R_j) = SAM(\mathbf{u}_i, \mathbf{u}_j) = \arccos\left(\frac{\sum_{b=1}^B u_{ib}u_{jb}}{[\sum_{b=1}^B u_{ib}^2]^{1/2}[\sum_{b=1}^B u_{jb}^2]^{1/2}}\right). \quad (1)$$

- If the regions have equal class labels  $L(R_i) = L(R_j) = k'$ ,

$$DC(R_i, R_j) =$$

$$(2 - \max(P_{k'}(R_i), P_{k'}(R_j)))DC_{spec}(\mathbf{u}_i, \mathbf{u}_j). \quad (2)$$

- If  $L(R_i) \neq L(R_j)$ , analyze region size: if a number of pixels in each region is larger than  $M$ ,  $DC(R_i, R_j) = \infty$ , otherwise:

$$DC(R_i, R_j) =$$

$$(2 - \min(P_{L(R_j)}(R_i), P_{L(R_i)}(R_j)))DC_{spec}(\mathbf{u}_i, \mathbf{u}_j). \quad (3)$$

Furthermore, for adjacent regions with non-equal class labels, their rectangularity features are analyzed. A region *rectangularity*  $rect(\cdot)$  is defined as a ratio of the region area and the area of a minimum area rectangle of an arbitrary orientation including the region. A set of classes *RecSet* representing objects with high rectangularity values is previously selected. Then, if

$$((card(R_r) > M) \& (L(R_r) \in RecSet) \& (rect(R_i \cup R_j) > rect(R_r))) = true, r \in \{i, j\},$$

Table 1: Results for the *Center of Pavia* image. Information Classes, Overall, Average and Class-Specific Accuracies in Percentage.

	SVM	ECHO	M-HSeg	HSegClas
Overall accuracy	94.96	95.11	96.35	<b>97.12</b>
Average accuracy	92.56	93.15	95.49	<b>97.03</b>
Water	98.12	<b>99.07</b>	97.74	97.62
Trees	90.48	93.43	90.36	<b>93.64</b>
Meadows	94.08	88.51	<b>95.62</b>	95.39
Bricks	79.86	82.84	87.77	<b>92.89</b>
Bare soil	97.12	94.96	<b>99.33</b>	99.01
Asphalt	93.52	92.31	95.01	<b>96.05</b>
Bitumen	82.48	92.57	94.80	<b>99.58</b>
Tile	97.41	96.21	98.80	<b>99.08</b>
Shadows	99.95	98.44	<b>100</b>	<b>100</b>

$$\text{then } DC(R_i, R_j) = W \cdot DC(R_i, R_j), \quad (4)$$

where  $card(R)$  is a number of pixels in the region  $R$ ,  $W$  is a user set parameter,  $W < 1$ . Once the dissimilarity criteria between all pairs of adjacent regions are computed, the algorithm proceeds as follows:

3) Find the smallest dissimilarity criterion value  $DC_{min}$ .

4) Merge all pairs of neighboring regions with  $DC = DC_{min}$ . For each new region  $R_{new} = R_i \cup R_j$  recompute:

- A vector of new class probabilities as

$$P_k(R_{new}) = \frac{P_k(R_i)card(R_i) + P_k(R_j)card(R_j)}{card(R_{new})}, \quad (5)$$

$k = 1, \dots, K$ ,  $card(R_{new}) = card(R_i) + card(R_j)$ .

- Class label as

$$L(R_{new}) = \arg \max_k \{P_k(R_{new})\}. \quad (6)$$

5) Stop if each image pixel has been involved at least once in the region merging procedure. Otherwise, update the dissimilarity criteria between the new regions and all regions spatially adjacent to them, and go to step 3.

## 3. Experimental results

The two most recent models (M-HSeg and HSegClas) are experimentally compared on the *Center of Pavia* image acquired by the Reflective Optics System Imaging Spectrometer. The image is of 785 by 300 pixels, with a spatial resolution of 1.3 m/pixel and 102 spectral channels. Nine thematic classes are considered, which are detailed in Table 1. Fig. 1(a) shows the reference data. Thirty samples for each class were randomly chosen from the reference data as training samples. The remaining samples composed the test set.

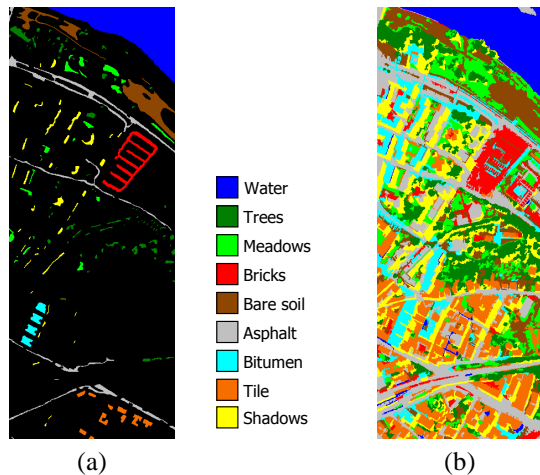


Figure 1: *Center of Pavia* image. (a) Reference data. (b) *HSegClas* classification map.

For both methods, one *versus* one SVM classification with the Gaussian radial basis function kernel was performed, with the parameters chosen by the five-fold cross validation:  $C = 128$  and  $\gamma = 2^{-5}$ . Other parameters were set as: for the M-Hseg method,  $M = 20$ ,  $P = 40\%$ ,  $S$  was set equal to the lowest probability within the highest 2% of probabilities; for the HSegClas method,  $M = 30$ ,  $W = 0.8$ , and  $RecSet = \{7, 8\}$ . Table 1 gathers overall, average and class-specific accuracies of the SVM, ECHO (Extraction and Classification of Homogeneous objects, a standard spectral-spatial classification technique in remote sensing) [13], M-HSeg and HSeg-Clas methods. As can be seen from the table, both hierarchical methods outperform the SVM and ECHO techniques. The HSegClas method yields the highest global and most of class-specific accuracies (see Fig. 1(b)).

#### 4. Conclusion

This paper overviewed hierarchical models for hyperspectral image classification. Experimental results did show that the recently developed spectral-spatial classification methods using hierarchical models succeed in taking advantage of both spatial and spectral information for accurate image analysis.

#### 5. References

- [1] C.-I. Chang, *Hyperspectral Data Exploitation: Theory and Applications*. Wiley-Interscience, 2007.
- [2] G. Camps-Valls and L. Bruzzone, "Kernel-based methods for hyperspectral image classification," *IEEE Trans. Geos. and Remote Sens.*, vol. 43, no. 6, pp. 1351–1362, June 2005.
- [3] L. Bruzzone and L. Carlin, "A multilevel context-based system for classification of very high spatial resolution images," *IEEE Trans. Geosc. and Remote Sens.*, vol. 44, no. 9, pp. 2587–2600, Sept. 2006.
- [4] Y. Tarabalka, J. C. Tilton, J. A. Benediktsson, and J. Chanussot, "A marker-based approach for the automated selection of a single segmentation from a hierarchical set of image segmentations," *IEEE JS-TARS*, vol. 5, no. 1, pp. 262–272, Feb. 2012.
- [5] M. Dalla Mura, A. Villa, J. Benediktsson, J. Chanussot, and L. Bruzzone, "Classification of hyperspectral images by using extended morphological attribute profiles and independent component analysis," *IEEE Geosc. and Remote Sens. Letters*, vol. 8, no. 3, pp. 542–546, May 2011.
- [6] A. Farag, R. Mohamed, and A. El-Baz, "A unified framework for MAP estimation in remote sensing image segmentation," *IEEE Trans. Geos. and Remote Sens.*, vol. 43, no. 7, pp. 1617–1634, July 2005.
- [7] J.-M. Beaulieu and M. Goldberg, "Hierarchy in picture segmentation: a stepwise optimization approach," *IEEE Trans. Pattern Analysis and Machine Intelligence*, vol. 11, no. 2, pp. 150–163, Feb 1989.
- [8] X. Huang and L. Zhang, "A comparative study of spatial approaches for urban mapping using hyperspectral ROSIS images over Pavia city, northern Italy," *Int. Journal of Remote Sens.*, vol. 30, no. 12, pp. 3205–3221, 2009.
- [9] S. v. d. Linden, A. Janz, B. Waske, M. Eiden, and P. Hostert, "Classifying segmented hyperspectral data from a heterogeneous urban environment using Support Vector Machines," *Journal of Applied Remote Sensing*, vol. 1, no. 1, 013543, 2007.
- [10] M. Baatz and A. Schape, "Multiresolution segmentation: an optimization approach for high quality multi-scale image segmentation," *Angewandte Geographische Informationsverarbeitung*, 2000.
- [11] Y. Tarabalka, J. A. Benediktsson, and J. Chanussot, "Classification of hyperspectral data using Support Vector Machines and adaptive neighborhoods," in *Proc. of the 6th EARSeL SIG IS workshop*, Tel Aviv, Israel, 2009, pp. 1–6.
- [12] Y. Tarabalka and J. C. Tilton, "Improved hierarchical optimization-based classification of hyperspectral images using shape analysis," in *Proc. of IGARSS'12*, Munich, Germany, 2012.
- [13] R. L. Kettig and D. A. Landgrebe, "Classification of multispectral image data by extraction and classification of homogeneous objects," *IEEE Trans. Geosc. Electr.*, vol. 14, no. 1, pp. 19–26, Jan. 1976.